

Journal of Geophysical Research: Atmospheres

RESEARCH ARTICLE

10.1002/2013JD020005

Key Points:

- WRF 4-D-Var is used to assimilate satellite-measured rainfall
- Sensitivity of WRF model forecast with strict and less strict quality control
- Improvement in WRF model forecast over Indian region

Correspondence to:
P. Kumar,
kam3545@gmail.com

Citation:
Kumar, P., C. M. Kishtawal, and P. K. Pal (2014), Impact of satellite rainfall assimilation on Weather Research and Forecasting model predictions over the Indian region, *J. Geophys. Res. Atmos.*, 119, 2017–2031, doi:10.1002/2013JD020005.

Received 10 APR 2013

Accepted 30 JAN 2014

Accepted article online 4 FEB 2014

Published online 3 MAR 2014

Impact of satellite rainfall assimilation on Weather Research and Forecasting model predictions over the Indian region

Prashant Kumar¹, C. M. Kishtawal¹, and P. K. Pal¹

¹Atmospheric and Oceanic Sciences Group, EPSA, Space Applications Centre (ISRO), Ahmedabad, India

Abstract Rainfall is probably the most important parameter that is predicted by numerical weather prediction models, though the skill of rainfall prediction is the poorest compared to other parameters, e.g., temperature and humidity. In this study, the impact of rainfall assimilation on mesoscale model forecasts is evaluated during Indian summer monsoon 2011. The Weather Research and Forecasting (WRF) model and its four-dimensional variational data assimilation system are used to assimilate the Tropical Rainfall Measuring Mission 3B42 and Japan Aerospace Exploration Agency Global Satellite Mapping of Precipitation retrieved rainfall. A total of five experiments are performed daily with and without assimilation of rainfall data during the entire month of July 2011. Separate assimilation experiments are performed to assess the sensitivity of WRF model forecast with strict and less strict quality control. Assimilation of rainfall improves the forecast of temperature, specific humidity, and wind speed. Domain average improvement parameter of rainfall forecast is also improved over the Indian landmass when compared with NOAA Climate Prediction Center Morphing technique and Indian Meteorological Department gridded rainfall.

1. Introduction

Rainfall is a highly variable parameter that varies in scales from few meters to several kilometers [Tustison *et al.*, 2003]. The importance of accurate rainfall observation and forecast are widely recognized. Rainfall forecast is one of the most crucial and least accurate outputs available from numerical weather prediction (NWP) models. Since rainfall affects society directly or indirectly, the accuracy and skill of rainfall prediction at varying spatiotemporal scales are strongly desirable. An assessment of the quality of the rainfall forecast is important to understand the strengths and deficiencies of current assimilation/forecast systems and also in view of future weather/climate projection. Rainfall forecast from the NWP models has improved over the last decades with the continuous progress in both numerical model and data assimilation techniques [Benedetti *et al.*, 2005; Bauer *et al.*, 2011; Lopez, 2011]. However, still there is a need to explore the new opportunities for model development through the use of data from active and passive sensors jointly [Benedetti *et al.*, 2005; Pu *et al.*, 2002; Bauer *et al.*, 2011]. Rainfall assimilation is considered as one of the important approaches to improve the weather forecasts, because rainfall observation includes the atmospheric information in terms of humidity, temperature, and winds and also contributes to the model atmospheric energy budget [Marecal and Mahfouf, 2003].

Several numerical modeling studies have shown that rainfall data improved the weather forecast [e.g., Bauer *et al.*, 2011; Krishnamurti *et al.*, 1991, 1993; Lopez, 2011; Puri and Miller, 1990; Treadon, 1996; Tsuyuki, 1997; Zou and Kuo, 1996; Zupanski and Mesinger, 1995]. A number of sensitivity tests have been performed for rainfall assimilation at various forecast/research centers like in European Centre for Medium-Range Weather Forecasts [Heckley *et al.*, 1990; Puri and Miller, 1990], Florida State University [Krishnamurti *et al.*, 1984, 1993; Tsuyuki, 1997], and National Centers for Environmental Prediction (NCEP) [Treadon, 1996, 1997]. For many fundamental reasons, rainfall assimilation is a more complex problem compared to assimilation of conventional or clear-sky satellite radiance [Errico *et al.*, 2007]. Marecal and Mahfouf [2000] demonstrated that nudging of rain rate improved the moisture analysis and reduced the spin-up problem. Due to sparse distribution of rain gauges and ground-based radars, satellite-retrieved precipitation is one of the major sources of rainfall observation. Treadon [1997] assimilated the satellite-retrieved rainfall rate in the NCEP three-dimensional variational (3-D-Var) data assimilation system. Rainfall assimilation using four-dimensional variational (4-D-Var) data assimilation method was first attempted by Zupanski and Mesinger [1995] using a

regional model. *Tsuyuki* [1997] tested the 4-D-Var assimilation of Special Sensor Microwave/Imager (SSM/I)-retrieved precipitation rates in global spectral model. Accurate rainfall observations at high spatial and temporal resolutions over tropical regions are possible only after the successful launch of the Tropical Rainfall Measuring Mission (TRMM) satellite [Pu *et al.*, 2002]. *Hou et al.* [2004] showed that assimilation of TRMM microwave imager (TMI) and SSM/I rainfall provided more accurate analysis and forecasts of the storm structures. Assimilation of TMI rainfall improves the global model analysis [*Hou et al.*, 2004] that subsequently impacts the mesoscale model forecasts, as the global model provides the initial and boundary conditions for the mesoscale model [Pu *et al.*, 2002]. Recently, rain rate assimilation became operational in 3-D-Var at the NCEP and in 4-D-Var at the Japan Meteorological Agency [Bauer *et al.*, 2011].

TRMM 3B42 and Japan Aerospace Exploration Agency (JAXA) Global Satellite Mapping of Precipitation (GSMap)-derived merged rainfall data are used in this study. The Weather Research and Forecasting (WRF) [Skamarock *et al.*, 2008] model and its 4-D-Var data assimilation [*Huang et al.*, 2009] system are used to assess the impact of rainfall assimilation in a regional forecast modeling framework over the Indian region of south central Asia. Due to non-Gaussian distribution of the rainfall observation, it is obligatory to evaluate the characteristics of strict (3 times the observation minus background departure) and less strict (5 times the observation minus background departure) quality control (QC) in data assimilation, which is one of the main objectives of this study. Additionally, merged rainfall products from TRMM 3B42 and JAXA GSMap are used in this study for both the cases of rain (when model rainfall value is greater than zero) and no-rain (when model rainfall value is equal to zero) over the entire domain compared to earlier studies in which swath data were used for assimilation. Preparation of separate background error covariance matrices for rain/no-rain cases is required for the rainfall assimilation, which may be the scope of future research. The following section 2 provides the details of rainfall data used for assimilation and validation. Details about the numerical model, rainfall data assimilation, design of experiments, and impact of rainfall assimilation on model analysis are discussed in section 3. Results are shown in section 4, while the last section summarizes the findings of the present study.

2. Rainfall Data

2.1. TRMM 3B42 Rainfall

The purpose of TRMM 3B42 rainfall product [*Huffman et al.*, 2007; *Haddad et al.*, 1997; *Adler et al.*, 2000] is to produce the merged infrared (IR) and microwave (MW) precipitation estimates. The TRMM 3B42 rainfall is sampled at $0.25^\circ \times 0.25^\circ$ spatial resolution with longitudinal global coverage extending from 50°S to 50°N latitude. The TRMM 3B42 rainfall is produced by a combination of passive MW data collected by TMI, SSM/I, Advanced Microwave Scanning Radiometer for EOS (AMSR-E) on board Aqua (not available since December 2011) and the advanced microwave sounding unit B (AMSU-B) on board the National Oceanic and Atmospheric Administration (NOAA) satellites. IR data measured from the international constellation of geosynchronous earth orbit (GEO) are calibrated with the precipitation estimate of precipitation radar and TMI combined algorithm. These data are averaged in case of multiple passes within 3 h time window for a given grid box [*Huffman et al.*, 2007]. A simple methodology has been adopted to combine the MW and IR estimates, and rain gauge data are used for correction over land [*Yuan et al.*, 2012].

2.2. JAXA GSMap Rainfall

JAXA GSMap is a high-resolution ($0.1^\circ \times 0.1^\circ$, hourly) satellite-based rainfall product similar to TRMM 3B42 rainfall. The objectives of the GSMap project are the development of an advanced microwave radiometer algorithm based on the deterministic rain retrieval algorithm and the generation of accurate high-resolution global product. JAXA GSMap is based on the combined MW-IR algorithm using TMI, AMSR-E on Aqua (not available since December 2011), SSM/I and AMSU, and IR from GEO. The estimates by passive microwave sensors are interpolated in time with the help of cloud moving vectors. The detailed information about GSMap can be obtained from *Okamoto et al.* [2005], *Kubota et al.* [2007], and *Aonashi et al.* [2009]. *Seto et al.* [2005] conducted a comparison between the GSMap products with other high-resolution precipitation products and rain gauge measurements over Japan. Results show that the algorithm has been improved in terms of rain classification methods over land.

2.3. Climate Prediction Center Morphing Technique Rainfall

The NOAA Climate Prediction Center Morphing technique (CMORPH) [Joyce *et al.*, 2004] uses the rainfall estimates from MW observations exclusively obtained from the low Earth-orbiting satellite. Currently, CMORPH incorporates the precipitation derived from passive MW aboard the SSM/I, AMSU-B, AMSR-E (not available since December 2011), and TMI. It is important to note that this technique is not a precipitation estimation algorithm but a means by which estimates from existing MW rainfall algorithms can be combined. Therefore, this method is extremely flexible such that any precipitation estimates from any MW satellite source can be incorporated.

3. WRF Model and Assimilation Methodology

3.1. WRF Model

Weather Research and Forecasting model version 3.4 is used in this study for short-range weather forecast. WRF model incorporates advance numerical techniques and two-way nesting and improves physics options which take care of convection and precipitation. The third-order Runge-Kutta scheme with smaller time step is used for acoustic and gravity wave modes. The physics options used in this study consist of WRF single-moment six-class for microphysics, the Kain-Fritsch [Kain and Fritsch, 1993] cumulus convection parameterization scheme, and the Yonsei University planetary boundary layer scheme [Hong and Pan, 1996]. The rapid radiative transfer model [Mlawer *et al.*, 1997] and Dudhia scheme [Dudhia, 1989] are used for longwave and shortwave radiation, respectively. Various sensitivity studies [Singh *et al.*, 2012; Kumar *et al.*, 2012] are performed to evaluate the performance of the above selected physics options over the Indian region.

3.2. Data Assimilation

The WRF 4-D-Var data assimilation system [Skamarock *et al.*, 2008; Huang *et al.*, 2009; Tsuyuki, 1997] is employed in this study to assimilate the rainfall observation. The 4-D-Var assimilation method uses the model dynamics to compute the model equivalent value at the valid report time of the observation. The major advantage of 4-D-Var is the use of full model dynamics to assimilate observation, having aims to provide better mesoscale weather forecast. The WRF 4-D-Var algorithm is based on incremental 4-D-Var formulation to find the analysis increment that minimizes a cost function. The WRF 4-D-Var includes the full nonlinear WRF model (WRF_NL) and the tangent linear and adjoint models of a simplified version of the nonlinear model. The nonlinear WRF model uses the full WRF dynamics, a large-scale condensation scheme, and a simple planetary boundary layer scheme (formulated as vertical diffusion plus surface friction). The transformation of algorithms in FORTRAN was used to construct the tangent linear model and its adjoint. The tangent linear and adjoint codes were verified using the standard gradient tests and tangent linear/adjoint tests procedure. A detailed description of the 4-D-Var system can be found in Huang *et al.* [2009].

We select a 6 h time window between 0000 UTC and 0600 UTC to assimilate the rainfall observation at 0600 UTC. The control variables are the stream function, velocity potential, unbalanced pressure, and relative humidity. Error correlations between control variables are neglected except for a constraint on mass and winds. Differences of 12 h and 24 h forecasts are used to determine the background error covariance matrix by National Meteorological Center method [Parrish and Derber, 1992]. In WRF 4-D-Var, observation errors are assumed as uncorrelated in both space and time. Since observation errors are assumed to be uncorrelated, the observational error covariance matrices are simple diagonal, with rainfall observation error as elements. Prakash and Gairola [2013] performed the validation of TRMM 3B42 with rain gauge measurements over the Indian region. Based on this study, 2 mm standard deviation is used as observation (here rainfall) error for 6 h duration. This observation error is considered as constant in space and time. Two different assimilation experiments based on QC are performed, in which rainfall observations that differed from the model first guess by more than either 3 (strict QC) or 5 (less strict QC) times the observational errors are removed. Accurate estimation of rainfall error is complex because of its high spatial and temporal variability. Therefore, two QC experiments using a strict and a less strict QC, respectively, are performed in this study. A fixed observation error is used here at all the grid points, although rainfall data have large spatial and temporal variability. If actual rainfall error is more (or less) than fixed observation error, assimilation system gives erroneously more (or less) weight to rainfall observation. So the use of constant observation error in this study represents a shortcoming that should be addressed in future studies.

Table 1. Assimilated Data in Numerical Experiments^a

Numerical Experiment	Data Used
CNT	No rainfall assimilation
JAXA strict (JAXAS)	JAXA rainfall with QC of 3 times the observation minus FG departure
JAXA less strict (JAXALS)	JAXA rainfall with QC of 5 times the observation minus FG departure
TRMM strict (TRMMS)	TRMM rainfall with QC of 3 times the observation minus FG departure
TRMM less strict (TRMMLS)	TRMM rainfall with QC of 5 times the observation minus FG departure

^aFG, first-guess.

3.3. Design of Numerical Experiments

A total of five experiments (Table 1) are performed daily with and without assimilation of rainfall (JAXA GSMAp and TRMM 3B42) data. Separate experiments (for 30 sample days) are performed with strict (3 times the observation minus background departure) and less strict (5 times observation minus background departure) QC. Observation minus background departure is the difference of the rainfall observation (accumulated rainfall between 0000 UTC and 0600 UTC) available from JAXA GSMAp or TRMM 3B42 and 6 h rainfall forecast (first-guess rainfall) from WRF model valid for same time period. For all the experiments, the model is integrated for 48 h starting from 0000 UTC during July 2011. WRF forecast experiments are conducted with a two-way nested domain, i.e., outer domain (domain 1: longitude: 32.1°E–111.9°E and latitude: 27.7°S–45.4°N) consisting of 150 × 150 grid points with 60 km horizontal grid resolution and inner domain (domain 2: longitude: 61.0°E–98.6°E and latitude: 2.8°N–37.4°N) consisting of 210 × 210 grid points with 20 km horizontal grid resolution (Figure 1). Rainfall assimilation is performed in the outer domain only, and two-way nesting is used to perform the model simulations, where domains at different grid resolutions are run simultaneously and communicate with each other. The coarser domain provides boundary value for the nest, and the nest feeds its calculation back to the coarser domain. The model has 36 vertical levels with top of the model atmosphere located at 10 hPa. NCEP Global Data Assimilation System (GDAS) analysis of 1° × 1° is used to prepare the lateral and low boundary conditions for all the experiments. NCEP GDAS analysis valid at 0000 UTC is used here as a first guess to evaluate the impact of rainfall assimilation because rainfall data available from TRMM 3B42 and JAXA GSMAp are not used directly in GDAS assimilation system [Bauer et al., 2011]. Six hours (between 0000 UTC and 0600 UTC) accumulated rainfall from TRMM and JAXA products is assimilated at 0600 UTC using WRF 4-D-Var assimilation system. Similar experiments (Table 1) are performed daily (for 30 sample days) where first guess is obtained from NCEP GDAS analysis. Use of accumulated rainfall observation for a given time window reduces both data volume and random errors compared to rain rate assimilation. All experiments are designed as a sequence of single assimilation cycles where only rainfall observation is used, with all other observations having already been assimilated by the NCEP GDAS system. In addition to this, two different merged rainfall products are used in this study, which contain the global gridded rainfall information from the combinations of MW and IR sensors, calibrated with rain gauge observations. These observations provide advantage of wide coverage and high temporal sampling compared to limited swath

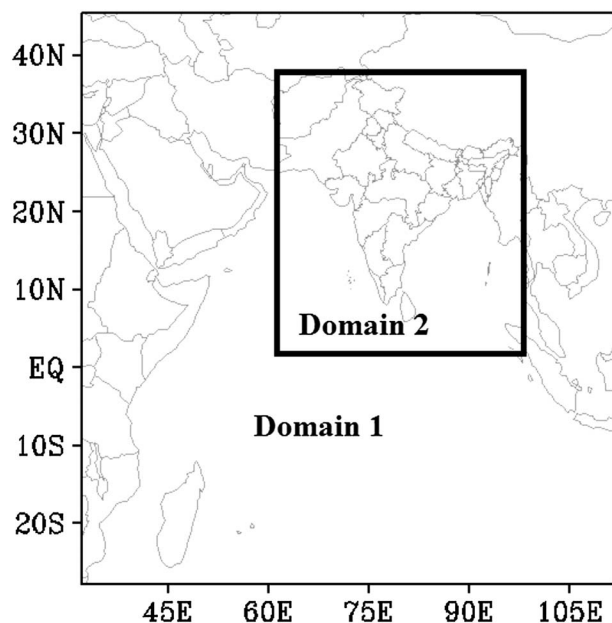


Figure 1. The nested domain used in WRF experiments. Domain 1 consists of 150 × 150 grid points with 60 km horizontal grid resolution, and domain 2 consists of 210 × 210 grid points with 20 km horizontal grid resolution.

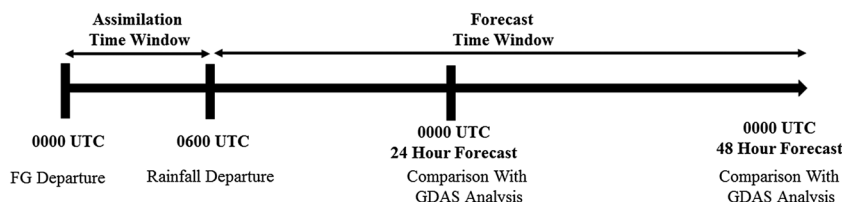


Figure 2. Schematic procedure to run the assimilation and forecast system. NCEP GDAS analysis is used as first guess at 0000 UTC, and rainfall data are assimilated at 0600 UTC. Thirty separate experiments are performed during July 2011.

observations from polar orbiting satellites. The schematic procedure to run the assimilation and forecast system is described in Figure 2.

3.4. Overview of the Fit to Rainfall

For the successful rainfall assimilation, the observation minus analysis ($O - A$; also known as analysis departure) is smaller than the observation minus background ($O - B$; also known as background departure). Figure 3 shows the background and analysis departure for less strict (TRMMLS) experiment during July 2011 (based on 30 assimilation experiments). The root-mean-square difference (RMSD) of first-guess (FG) (Figure 3a) and analysis (Figure 3b) rainfall departure is 2.24 mm and 1.33 mm, respectively (Table 2), at 0600 UTC during 1–30 July 2011. The mean difference is reduced from -0.48 mm ($O - B$) to 0.02 mm ($O - A$). In case of strict (TRMMS) experiments (Table 2), the mean difference is reduced from -0.33 mm ($O - B$) to -0.01 mm ($O - A$), while RMSD is decreased from 1.46 mm to 0.95 mm. Rainfall forecast from WRF analyses is closer to the rainfall observation compared to rainfall forecast from first guess. These results confirm the successful assimilation of TRMM 3B42 rainfall observations. Similar results are obtained when JAXA GSMaP rainfall observations are used for data assimilation experiments (Table 2). Slightly smaller RMSD is observed in JAXA experiments compared to those in TRMM experiments.

Spatial distribution of TRMM 3B42 rainfall and corresponding rainfall forecast from WRF analysis valid at 0600 UTC 1 July 2011 are shown in Figure 4. Figures 4a and 4d display the rainfall data assimilated in strict (TRMMS) and less strict (TRMMLS) QC experiments. The WRF rainfall forecast is able to capture the rainy location of northeast India, Punjab, and Arabian Sea. However, it must be pointed out that there are a few regions where the model forecasts rainfall (see Figures 4b and 4e), while the observations (see Figures 4a and 4d) indicate that they are in fact nonrainy regions. Difference of observed rainfall and 6 h rainfall forecast (rainfall generated at the end of assimilation window) for strict and less strict QC are shown in Figures 4c and 4f, respectively. Due to non-Gaussian distribution of rainfall errors, differences are more in less strict QC experiments compared to TRMMS experiments. Similar features are observed in case of JAXA rainfall assimilation experiments. After rainfall assimilation, 6 h rainfall forecast from WRF analyses are improved (figure not shown) when compared with observed TRMM rainfall.

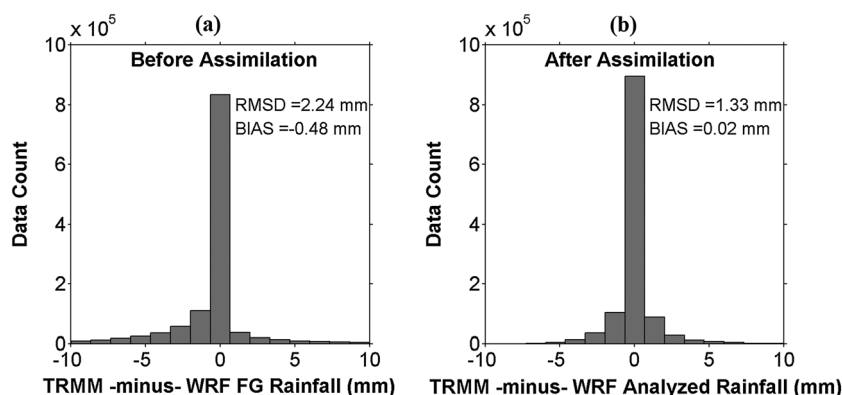


Figure 3. Histogram of (a) TRMM 3B42 rainfall minus WRF first-guess rainfall (mm) and (b) TRMM 3B42 rainfall minus WRF analyzed rainfall (mm) at 0600 UTC during the entire month of July 2011.

Table 2. Error in Fit of Rainfall Observations

Experiment		JAXAS	JAXALS	TRMMS	TRMMLS
Bias (mm)	Background Departure	-0.46	-0.67	-0.33	-0.48
	Analysis Departure	-0.02	-0.02	-0.01	0.02
RMSD (mm)	Background Departure	1.41	2.2	1.46	2.24
	Analysis Departure	0.85	1.23	0.95	1.33

3.5. Impact of Rainfall Assimilation on WRF Analysis

Spatial distribution of mean deviation for specific humidity analysis (rainfall assimilation experiment—CNT experiment) at 850 hPa is shown in Figure 5. Large differences in specific humidity are observed over Western Ghats (mountain range along the western side of southern India), northern India, and northeast part of India in JAXA-based experiments (JAXAS, Figure 5a; and JAXALS, Figure 5b). JAXA-based experiments show less moisture compared to CNT experiment over these regions. These deviations are more significant in JAXALS analysis over Western Ghats. In comparison to JAXA experiments, TRMMS (Figure 5c) and TRMMLS (Figure 5d) analyses have less difference with CNT analysis over northern India and northeast part of India. Decrease in high-moisture region is observed over the Arabian Sea, Bay of Bengal, northeast India, and Gangetic Plain after rainfall assimilation. Very less or no changes are observed over the rain shadow region of the eastern coast of southern peninsular India and in the Indian Ocean. Similar to specific humidity analysis, reduction in temperature analysis (figure not shown) is also observed over the Indian landmass, Bay of Bengal, and Arabian Sea after rainfall assimilation. It is expected that elimination of observations (here rainfall) differing by large amount from the rainfall forecast from first guess (first-guess rainfall) in strict QC reduces the influence of the rainfall data, which agree with the results obtained above.

4. Results and Discussions

In this paper, we use mean difference (bias) and root-mean-square difference (RMSD) as the standard statistical parameter to evaluate the WRF model forecast for domain 2 (Figure 1). Model-predicted temperature, humidity, and winds are compared with NCEP GDAS analysis and in situ observations to compute the error statistics. Rainfall forecast is validated with CMORPH rainfall and India Meteorological Department (IMD; over land)

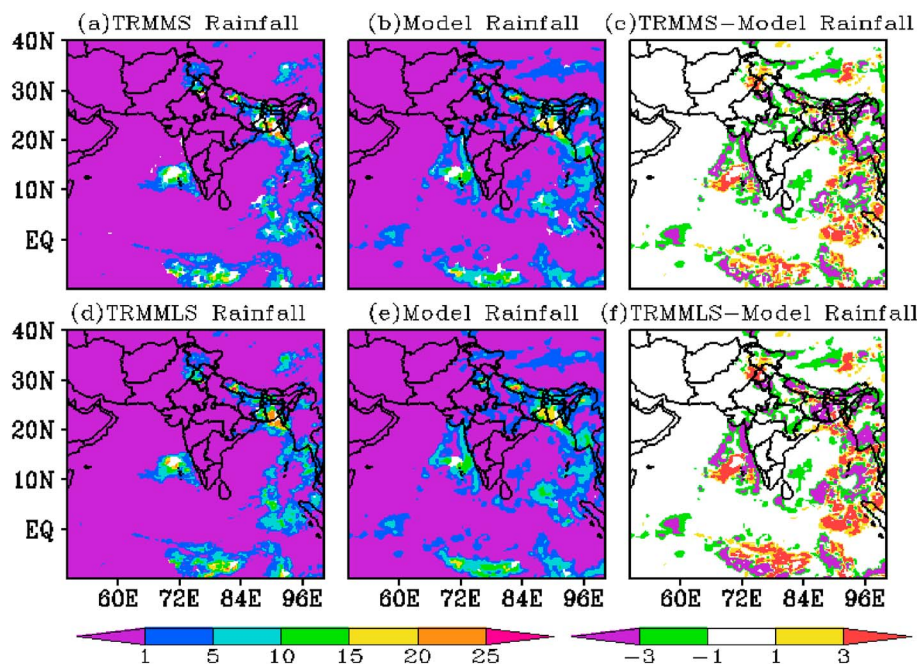


Figure 4. Spatial distribution of (a) TRMM rainfall used in strict QC assimilation experiment, (b) model rainfall from TRMMS experiment, (c) TRMMS minus model rainfall, (d) TRMM rainfall used in less strict QC assimilation experiment, (e) model rainfall from TRMMLS experiment, and (f) TRMMLS minus model rainfall on 1 July 2011 (assimilation window is 0000 UTC to 0600 UTC).

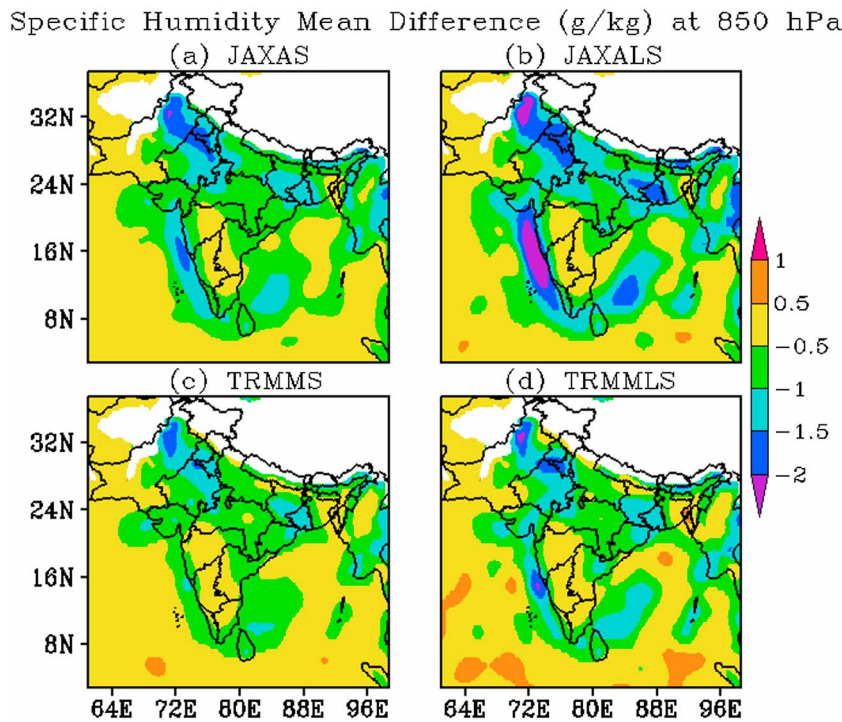


Figure 5. Spatial distribution of mean difference in (a) JAXAS, (b) JAXALS, (c), TRMMS, and (d) TRMMLS analyzed specific humidity minus specific humidity from control experiment at 850 hPa during the entire month of July 2011.

observed gridded rainfall [Rajeevan *et al.*, 2006]. The improvement parameter (δ ; equation (1)) is used to quantify the improvement in the forecast due to rainfall assimilation,

$$\delta = \frac{\left[\frac{1}{N} \sum_{i=1}^N (O_i - C_i)^2 \right]^{1/2} - \left[\frac{1}{N} \sum_{i=1}^N (O_i - E_i)^2 \right]^{1/2}}{\left[\frac{1}{N} \sum_{i=1}^N (O_i - C_i)^2 \right]^{1/2}} \times 100 \quad (1)$$

where “C” is the forecast predicted from CNT experiment (without rainfall assimilation), “E” is the forecast produced from rainfall assimilation experiments, “O” is the observation, and N is the total number of forecasts, which are 30 in this case. The improvement parameter is calculated for each grid point. A positive (negative) value of improvement parameter indicates the improvement (degradation) in the forecast due to rainfall assimilation compared to control experiment.

4.1. Temperature

Spatial distribution of improvement parameter (equation (1)) in 24 h temperature forecast at lower level (850 hPa) is shown in Figure 6. More than 10% improvement is observed in most of the locations. Higher than 20% improvement parameter is also seen in some regions like Bay of Bengal and western India. Few pockets of very less improvement or degradation are also observed over central and southern India. Domain average value of improvement parameter is 13.7%, 13.6%, 12.1%, and 11.8% for JAXAS, JAXALS, TRMMS, and TRMMLS experiments, respectively. It shows that not much difference is seen in JAXA-based experiments when less strict and strict QC is used. Moreover, the number of grid points showing improvements is higher in strict QC experiments compared to less strict QC experiments. In strict QC experiments, 39,122 (88.7%) and 37,866 (85.9%) grid points showing improvement in JAXAS and TRMMS experiments, respectively, which decrease to 38,464 (87.2%) and 37,349 (84.7%) when less strict QC are used. Positive impact is slightly reduced when less strict QC is used for TRMM assimilation experiments. Spatial distribution of Student’s *t* test (figure not shown) based on 30 samples during July 2011 reveals that more improvement/degradation in less strict QC (TRMMLS and JAXALS) experiments is statistically significant (at 95% confidence level) over southern India compared to

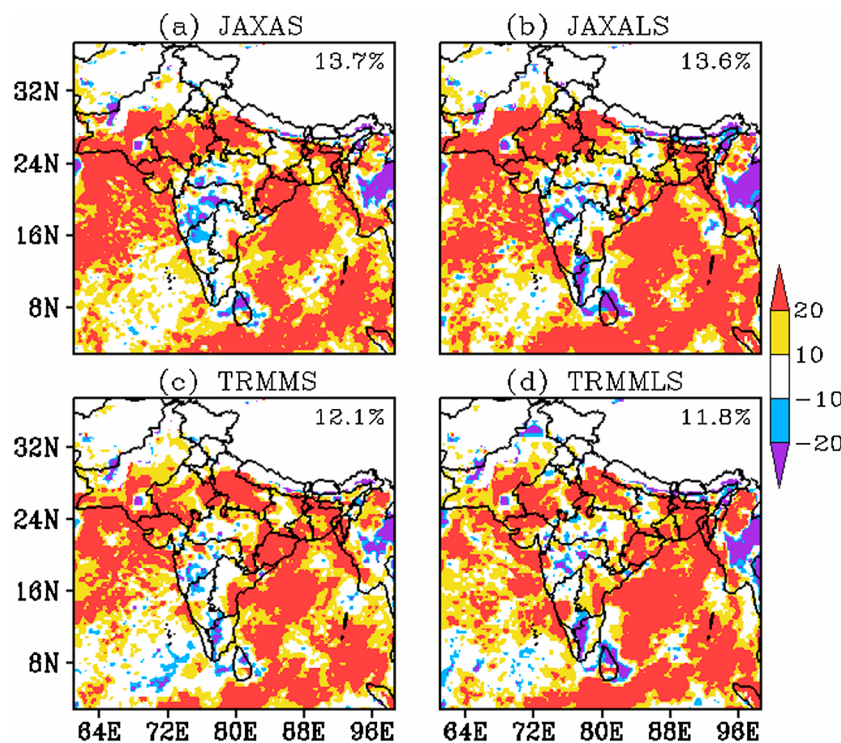


Figure 6. Spatial distribution of improvement parameter in 24 h temperature forecast at 850 hPa from (a) JAXAS, (b) JAXALS, (c) TRMMS, and (d) TRMMLS experiments compared to control experiment. Domain average value of improvement parameter is also shown in the figure.

strict QC (TRMMS and JAXAS) experiments. Additionally, 24 h (at 850 hPa; Figure 6) temperature forecast show more positive impact in JAXA-based experiments (~13.7%) compared to TRMM-based experiments (~12.0%). This higher positive impact in JAXA experiments may be due to the availability of high-spatial-resolution rainfall data that improve the finer-scale representation of near-surface physical processes that eventually lead to improved prediction of low-level temperature. In addition to this, less RMSD error is observed in JAXA analysis compared to that in TRMM analysis. Overall, domain average improvement parameter shows that 24 h temperature forecast is improved after rainfall assimilation compared to that in the control experiment.

Spatial distribution of improvement parameter for 48 h temperature forecast at 850 hPa is shown in Figure 7. Similar to 24 h temperature forecast, rainfall assimilation experiments show the improvement over the Arabian Sea, Bay of Bengal, northeast India, and Gangetic plains. Few pockets of degradation are also seen over Central India. Assimilation experiments with less strict QC (TRMMLS and JAXALS) show more improvement compared to strict QC (TRMMS and JAXAS) experiments. Domain average value of improvement parameter is increased from 7.2% (JAXAS) and 5.6% (TRMMS) in strict QC experiments to 9.5% (JAXALS) and 6.7% (TRMMLS) in less strict QC experiments. Spatial distribution of Student's *t* test (figure not shown) also demonstrate that more improvement in less strict QC experiments compared to strict QC experiments is statistically significant at 95% confidence level over northern India. The number of grid points representing improvement is decreased in 48 h forecast compared to that in 24 h forecast. Approximately 85% grid points represent the improvement in 48 h temperature forecast. It is interesting to note here that in the 24 h temperature forecast, strict QC experiments show more positive impact compared to less strict QC experiments, but as the forecast length is increased from 24 h to 48 h, less strict QC experiments show more skill compared to strict QC experiments. The possible reason may be that in the case of strict QC experiments, less number of rainfall observations are used for assimilation whose impact is reduced as the forecast length is increased. Due to significant changes in initial condition of less strict QC experiments, rainfall assimilation influences the long-term forecast also. In both the cases, JAXA-based experiments show more improvement compared to TRMM-based experiments.

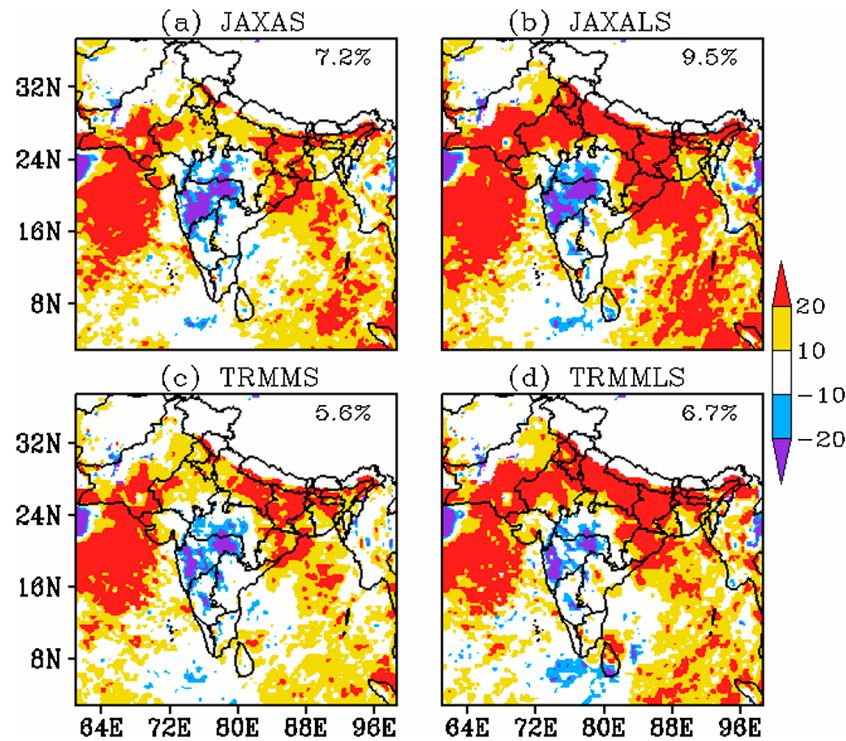


Figure 7. Spatial distribution of improvement parameter in 48 h temperature forecast at 850 hPa from (a) JAXAS, (b) JAXALS, (c) TRMMS, and (d) TRMMLS experiments compared to control experiment. Domain average value of improvement parameter is also shown in the figure.

Vertical profile of domain average RMSD and improvement parameter (equation (1)) for 24 h temperature forecast are shown in Figure 8. Maxima of 1.3°C, 1.1°C, and 1.7°C RMSD (Figure 8a) are observed in 24 h temperature forecast in lower levels (1000–700 hPa), midlevels (650–150 hPa), and upper levels (100–50 hPa), respectively. Rainfall assimilation-based experiments have less error compared to control experiments. Positive improvement in different vertical levels of temperature forecast may be due to the multivariate nature of WRF 4-D-Var system, which improves the model initial condition and further model forecasts. Approximately 10% improvement (Figure 8b) is observed in temperature forecast at 900–600 hPa, whereas no improvement or degradation is observed in upper layers. TRMMS experiments show slightly more improvement in 24 h temperature forecast compared to TRMMLS experiments. More degradation in upper level (200 hPa) forecast is observed in JAXA-based experiments compared to TRMM-based experiments. Overall, in lower levels and midlevels (700–400 hPa), strict QC experiments show more skill in temperature forecast. Above 300 hPa, strict QC show more degradation against control experiments.

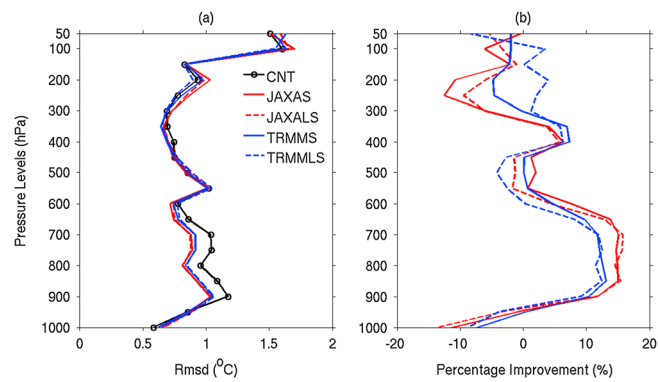


Figure 8. Vertical profile of domain average (a) RMSD and (b) improvement parameter of 24 h temperature forecast from all the experiments.

In lower vertical levels, JAXA experiments have more positive impact compared to TRMM-based experiments.

Six-hourly surface (2 m) temperature forecast (Figure 9) is also compared with surface observations available from NCEP Global Telecommunications System. A diurnal pattern is observed in RMSD which show maximum error in surface temperature forecast at 1200 UTC, whereas minimum RMSD error is observed at 0000 UTC. It illustrates that this model is inefficient to predict the maximum value of temperature. The maximum mean RMSD error over

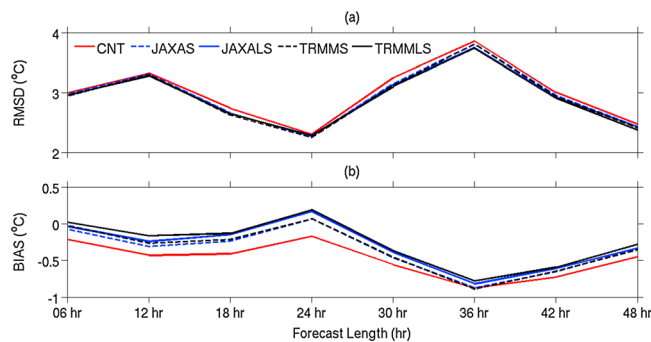


Figure 9. Domain average (a) RMSD and (b) bias of 2 m air surface temperature with in situ observations for all the experiments.

the 48 h forecasts is close to 4°C and occurs at 36 h forecast. It is interesting to note that in up to 30 h surface temperature forecast, no significant differences are observed in strict and less strict QC experiments. In 36 h surface temperature forecasts, less strict QC experiments show better forecasts compared to strict QC experiments. In most of the forecast hours, bias reduction is more in less strict QC experiments compared to strict QC experiments which show that additional rainfall observations used in

less strict QC assimilation experiments have positive impact on near-surface temperature forecast. In all the cases, rainfall assimilation improved the surface temperature forecast; no significant differences are observed in JAXA and TRMM rainfall data assimilation experiments.

4.2. Humidity

Spatial distribution of improvement parameter in 48 h surface (2 m) specific humidity forecast is shown in Figure 10. Rainfall assimilation experiments show positive impact over the Bay of Bengal and Arabian Sea. Few pockets of degradation in specific humidity forecast are also observed in rainfall assimilation experiments over Central India and Gangetic Plain compared to the control run. Assimilation experiments with less strict QC (TRMMLS and JAXALS) show more impact (improvement or degradation) compared to strict QC experiments (TRMMS and JAXAS) in 48 h surface humidity forecast. Domain average improvement parameter shows more improvement in JAXA experiments (3.7 and 4.2% in strict and less strict QC, respectively) compared to TRMM experiments (3.0 and 3.6% in strict and less strict QC, respectively) in 48 h surface specific

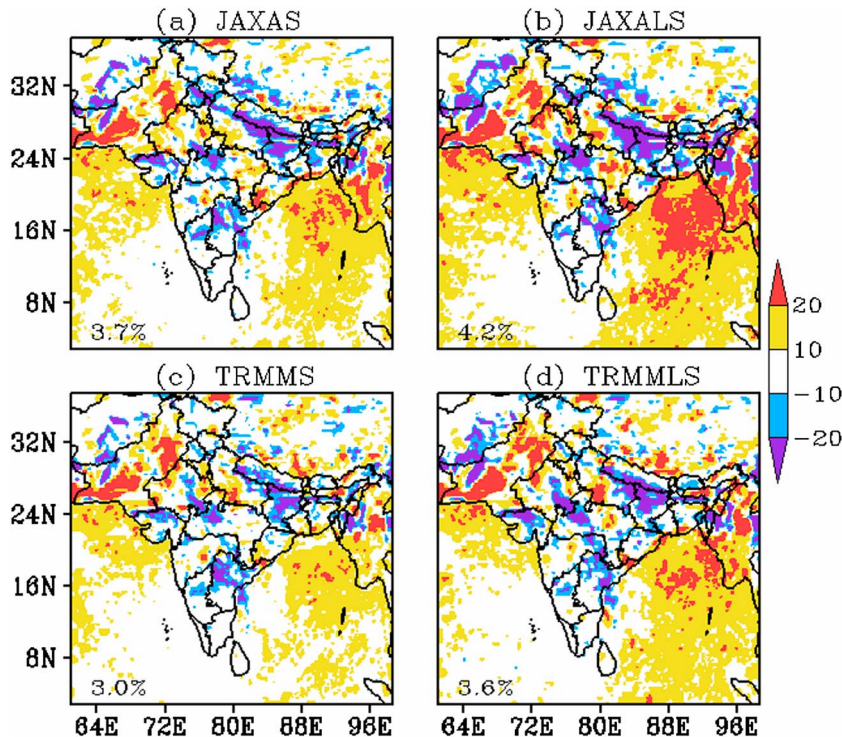


Figure 10. Spatial distribution of improvement parameter in 48 h surface specific humidity forecast from (a) JAXAS, (b) JAXALS, (c) TRMMS, and (d) TRMMLS experiments compared to control experiment. Domain average value of improvement parameter is also shown in the figure.

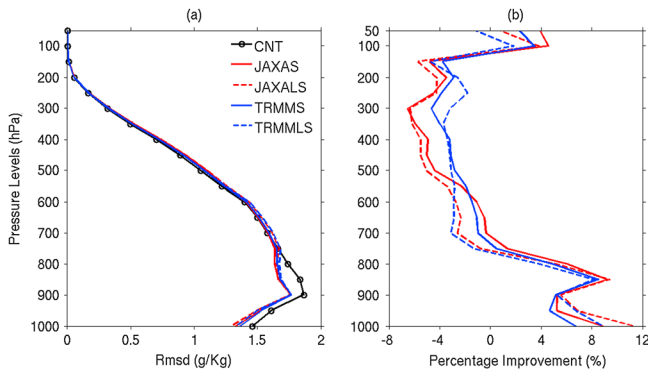


Figure 11. Vertical profile of domain average (a) RMSD and (b) improvement parameter of 48 h specific humidity forecast from all the experiments.

less strict QC experiments in 24 h forecast. Moreover, similar to temperature forecast, it is observed that 48 h surface specific humidity forecast is improved when less strict QC is used in place of strict QC experiments. In case of TRMM data assimilation, ~68% grid points represent the improvement in 48 h surface specific humidity forecast in strict QC experiments which increase to ~70% in less strict QC experiments. Again, it is important to note here that JAXA-based experiments have more positive skill in comparison to TRMM rainfall assimilation experiments.

Vertical profile of domain average RMSD and improvement parameter for 48 h specific humidity forecast are shown in Figure 11. Maxima of 1.8 g/kg, 1.5 g/kg, and 0.7 g/kg RMSD (Figure 11a) are observed in lower levels (1000–700 hPa), midlevels (650–400 hPa) and upper levels (350–50 hPa), respectively. Rainfall assimilation-based experiments have less error in lower levels (1000–800 hPa) compared to control experiment. Approximately 8% improvement (Figure 11b) is observed in lower levels, whereas less improvement or degradation is observed in remaining vertical layers. It is important to note here that JAXA-based experiments have more degradation in upper levels compared to TRMM-based experiments. All the rainfall assimilation experiments show degradation in moisture forecast at upper level; this degradation is more intense in JAXA experiments. TRMMLS and JAXALS experiments show more positive improvement compared to TRMMS and JAXAS experiments, respectively, in 48 h moisture forecast (at 1000 hPa).

4.3. Winds

Daily domain average RMSD for surface (10 m) wind speed forecast is shown in Figure 12. Approximately 2.4 m s^{-1} RMSD (Figure 12a) is observed in 48 h surface wind speed forecast. Rainfall assimilation experiments have less RMSD compared to CNT experiment. A consistent reduction in bias (Figure 12b) is observed in rainfall assimilation experiments. All the rainfall assimilation experiments show a similar kind of improvement in 48 h surface wind speed forecast. Similar to previous results, less strict QC experiments show better results in 48 h wind speed forecast. The vertical profile of domain average RMSD of wind speed (figure not shown) shows that

humidity forecast. Again, it is found that in 24 h surface specific humidity forecast (figure not shown), strict QC experiments improve the forecast compared to less strict QC experiments. Approximately 67% and 64% grid points represent the improvement in JAXAS and TRMMS experiments, respectively, which decrease to 64.7% and 61.7% improvement in less strict QC experiments. These findings are again similar to those of previous studies which show that strict QC is advantageous in case of rainfall assimilation experiments compared to

less strict QC experiments in 24 h forecast. Moreover, similar to temperature forecast, it is observed that 48 h surface specific humidity forecast is improved when less strict QC is used in place of strict QC experiments. In case of TRMM data assimilation, ~68% grid points represent the improvement in 48 h surface specific humidity forecast in strict QC experiments which increase to ~70% in less strict QC experiments. Again, it is important to note here that JAXA-based experiments have more positive skill in comparison to TRMM rainfall assimilation experiments.

Approximately 8% improvement (Figure 11b) is observed in lower levels, whereas less improvement or degradation is observed in remaining vertical layers. It is important to note here that JAXA-based experiments have more degradation in upper levels compared to TRMM-based experiments. All the rainfall assimilation experiments show degradation in moisture forecast at upper level; this degradation is more intense in JAXA experiments. TRMMLS and JAXALS experiments show more positive improvement compared to TRMMS and JAXAS experiments, respectively, in 48 h moisture forecast (at 1000 hPa).

4.4. Rainfall

Verification of rainfall forecasts is essential to evaluate the performance of weather models which provide useful feedback for further improvements. For the verification of rainfall forecast,

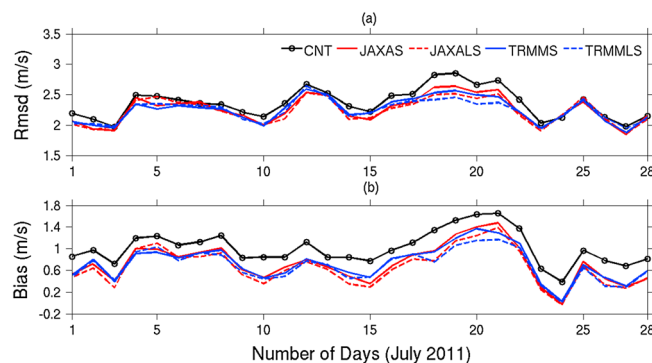


Figure 12. Time series of (a) RMSD (m/s) and (b) bias of 48 h surface (10 m) wind speed forecast from all the experiments.

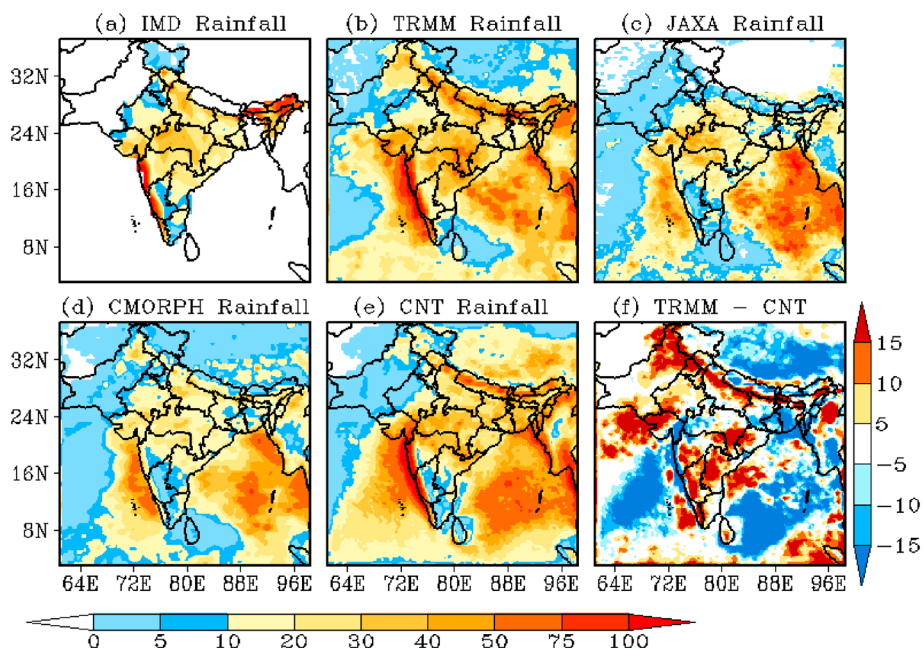


Figure 13. Spatial distribution of monthly rainfall from (a) IMD gridded rainfall, (b) TRMM 3B42 rainfall, (c) JAXA GSMP rainfall, (d) CMORPH rainfall, (e) 24 h rainfall forecast from CNT experiment, and (f) TRMM minus CNT rainfall during July 2011.

CMORPH precipitation analyses at $0.25^\circ \times 0.25^\circ$ spatial and 3-hourly temporal resolutions are used in this study. The model-predicted rainfall is resampled to $0.25^\circ \times 0.25^\circ$ using bilinear interpolation. The model-predicted rainfall (regridded at $1^\circ \times 1^\circ$ resolution) is also compared with IMD gridded rainfall over land.

The monthly (July 2011) rainfall from IMD (Figure 13a) and TRMM (Figure 13b) shows that the maximum monsoon rainfall is observed over the west coast of peninsular India and over the northeast region. Less rainfall is observed over northern India and rain shadow region of the east coast of southern peninsular India during Indian summer monsoon 2011. JAXA monthly rainfall (Figure 13c) also shows the similar spatial distribution of rainfall, but it misses the orography-induced rainfall due to lack of surface observations (rain gauge correction) in these products. Similar to JAXA rainfall, less rainfall is observed in CMORPH monthly rainfall (Figure 13d) over rain shadow region of southern India. Northern India also shows less rainfall value in CMORPH product compared to TRMM monthly rainfall. The accumulated 24 h rainfall forecast from CNT experiment is shown in Figure 13e. The difference of accumulated rainfall from TRMM and 24 h rainfall forecast from CNT experiment (Figure 13f) shows that CNT underpredicted the rainfall in western and northern parts of India and overestimated the rainfall in Western Ghats, eastern India, Arabian Sea, and Bay of Bengal.

For the quantitative assessment of improvement (degradation) in rainfall forecast, we compute the spatial distribution of ($\text{RMSD}_{\text{CNT}} - \text{RMSD}_{\text{ASS}}$). Figure 14 shows the improvement in 24 h rainfall forecast in assimilation experiments compared to control experiment. Figure 14 reveals that the implementation of rainfall assimilation improves the rainfall prediction over the Indian landmass and the Bay of Bengal region with large improvements over the mountainous region (Himalayan). This better rainfall prediction is probably due to the improved prediction of temperature and moisture. Slightly less improvement is observed in less strict QC experiments (55% and 52% grid points improved in JAXALS and TRMMLS, respectively) compared to strict QC experiments (61% and 59.9% grid points improved in JAXAS and TRMMS, respectively). Marginally higher improvement is observed in JAXA-based experiments compared to TRMM-based experiments. Spatial distribution of improvement parameter for rainfall forecast when compared with IMD gridded rainfall over the Indian landmass is shown in Figure 15. The 24 h rainfall forecast is improved (Figure 15; relative to the control simulation) over the west coast of India, southern India, and eastern India. Degradation in improvement parameter is observed when less strict QC is used for data assimilation. Domain average improvement parameter in 24 h rainfall forecast is 8%, 4.3%, 5.1%, and 2.7% in JAXAS, JAXALS, TRMMS, and TRMMLS experiments, respectively. Again, it is observed that JAXA experiments have more positive impact on 24 h rainfall forecast.

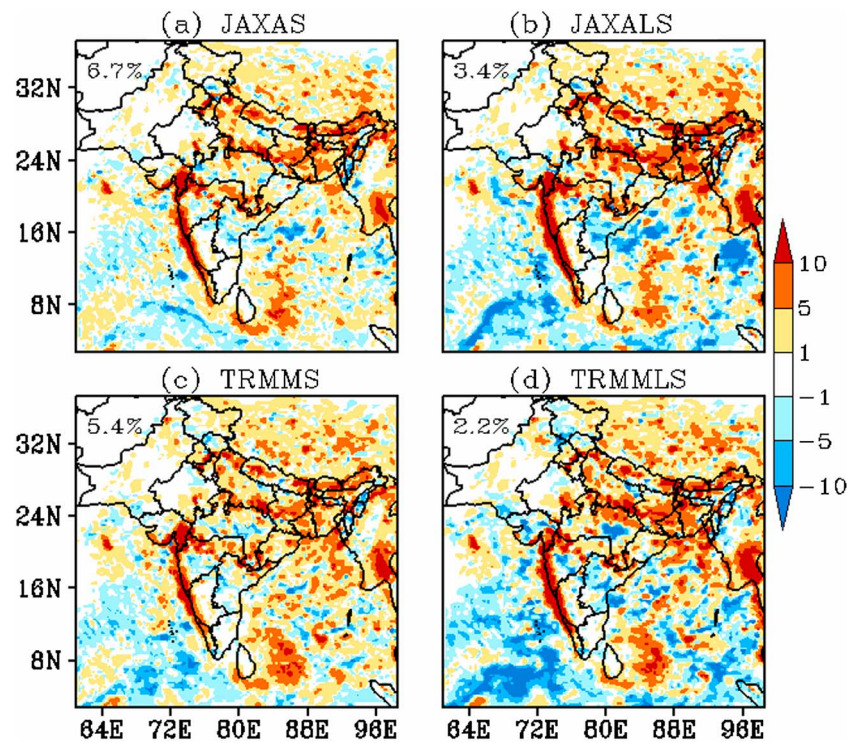


Figure 14. Spatial distribution of improvement in 24 h rainfall forecast from (a) JAXAS, (b) JAXALS, (c) TRMMMS, and (d) TRMMLS experiments over control experiment when compared with CMORPH rainfall. Domain average value of improvement parameter is also shown in the figure.

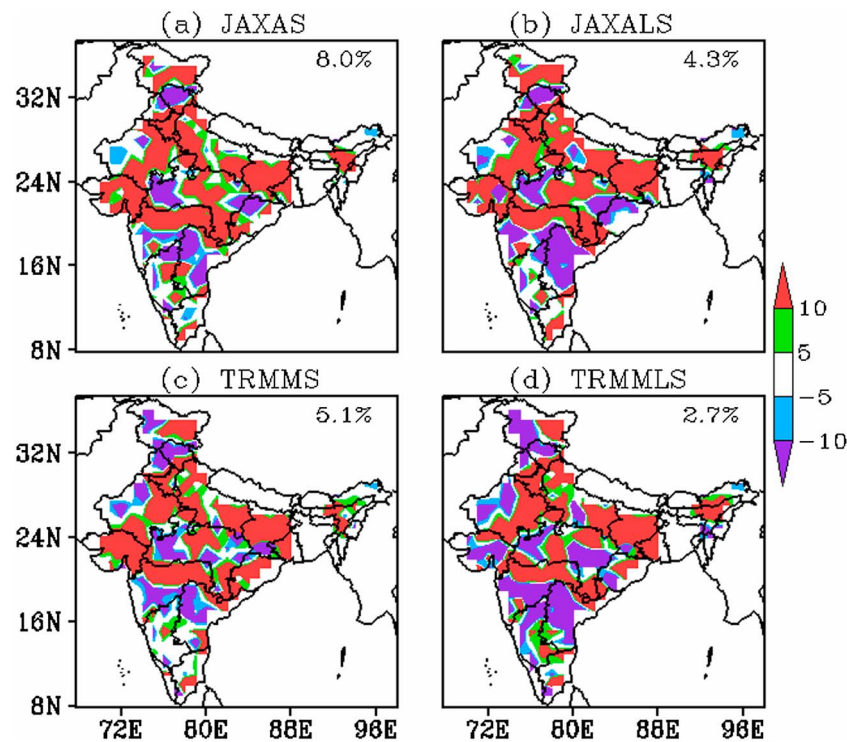


Figure 15. Spatial distribution of improvement parameter in 24 h rainfall forecast from (a) JAXAS, (b) JAXALS, (c) TRMMMS, and (d) TRMMLS experiments over control experiment when compared with IMD gridded rainfall over Indian landmass. Domain average value of improvement parameter is also shown in the figure.

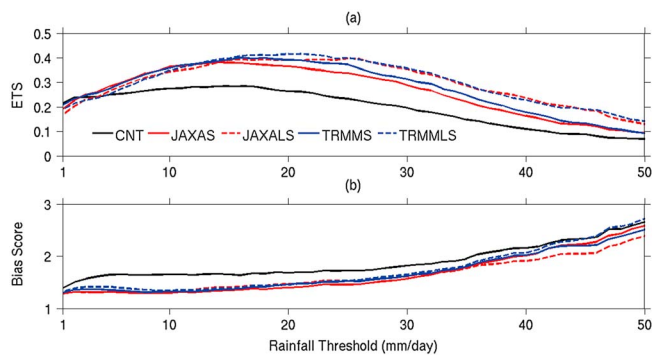


Figure 16. (a) Equitable threat score (ETS) and (b) bias score in 24 h rainfall prediction with corresponding CMORPH observations for different rainfall thresholds.

data as observed rainfall for different rainfall thresholds. In comparison to CMORPH rainfall, all experiments (Table 1) overestimated the rainfall (bias score is more than 1). The rainfall prediction skill is improved (higher ETS and lower bias; Figure 16) after rainfall assimilation. When strict QC is used, TRMM-based experiments show more skill compared to JAXA experiments for high rainfall thresholds. However, no significant differences are observed in two different rainfall assimilation experiments when less strict QC is used. Less strict QC experiments degrade the rainfall forecast for less rainfall threshold (12 mm/d) and show better skill at higher rainfall thresholds. Overall, based on rainfall forecast verification, which is one of the important parameters, we can conclude that rainfall assimilation has positive impact over the Indian region during the monsoon period.

5. Conclusion

In this study, WRF model has been used to assimilate the rainfall data during Indian summer monsoon 2011. To assimilate the TRMM 3B42 and JAXA GSMAp rainfall with strict and less strict QC, 4-D-Var data assimilation method is used. Rainfall assimilation improves the low-level temperature, moisture, and wind speed forecast. Results also show that rainfall assimilation improves the rainfall forecast. Large improvements are observed when JAXA GSMAp rainfall is used for assimilation compared to TRMM experiments. This higher positive impact in JAXA-based experiments may be due to the availability of high-spatial-resolution rainfall data. It is interesting to note here that in the first 24 h forecast, strict QC improves the forecast of temperature, moisture, winds, etc. But as the forecast length is increased from 24 h to 48 h, less strict QC experiments have more improvement compared to strict QC experiments. In this study, model analysis is also improved when no-rain information is used for assimilation which motivates the future research to use separate background error for precipitating and nonprecipitating regions. Thus, assimilating the rainfall observation in the WRF model can be viewed as a positive step toward improving the accuracy of mesoscale numerical modeling for short-range weather forecast.

Acknowledgments

The authors would like to thank A.S. Kiran Kumar, Director, SAC; and J.S. Parihar, Deputy Director, EPSA/SAC for constant encouragement and guidance. Authors are thankful to the NCAR for the WRF model. We are thankful to NASA for the valuable data from TRMM website <http://disc2.nascom.nasa.gov/Giovanni/tovas>. Authors are also thankful to JAXA GSMAp and CMORPH for providing high-resolution rainfall observations. The authors are grateful for comments and suggestions by anonymous reviewers that helped to improve the quality of this paper.

To examine the performance of WRF model in predicting the frequency of rainfall occurrence events at or above a particular precipitation threshold, we also compute the statistical skill scores (bias scores (BSs) and equitable threat scores (ETSs)) for 24 h accumulated rainfall. These statistics are obtained by comparing 30 samples of daily accumulated rainfall from all the five experiments with corresponding observed CMORPH rainfall at various rainfall thresholds. Figure 16 shows the ETS and BS statistics using CMORPH

References

- Adler, R. F., D. T. Bolin, S. Curtis, and E. J. Nelkin (2000), Tropical rainfall distributions determined using TRMM combined with other satellite and rain gauge information, *J. Appl. Meteorol.*, **39**, 2007–2023.
- Aonashi, K., et al. (2009), GSMAp passive, microwave precipitation retrieval algorithm: Algorithm description and validation, *J. Meteorol. Soc. Jpn.*, **87A**, 119–136.
- Bauer, P., et al. (2011), Satellite cloud and precipitation assimilation at operational NWP centres, *Q. J. R. Meteorol. Soc.*, **137**, 1934–1951.
- Benedetti, A., P. Lopez, P. Bauer, and E. Moreau (2005), Experimental use of TRMM precipitation radar observations in 1D + 4D – Var assimilation, *Q. J. R. Meteorol. Soc.*, **131**(610), 2473–2495.
- Dudhia, J. (1989), Numerical study of convection observed during the winter monsoon experiment using a mesoscale two-dimensional model, *J. Atmos. Sci.*, **46**, 3077–3107.
- Errico, R. M., P. Bauer, and J. F. Mahfouf (2007), Issues regarding the assimilation of cloud and precipitation data, *J. Atmos. Sci.*, **64**, 3785–3798.
- Haddad, Z. S., E. A. Smith, C. D. Kummerow, T. Iguchi, M. R. Farrar, S. L. Durden, M. Alves, and W. S. Olson (1997), The TRMM day-1 radar/radiometer combined rain-profiling algorithm, *J. Meteorol. Soc. Jpn.*, **75**, 799–809.
- Heckley, W. A., G. Kelly, and M. Tiedtke (1990), On the use of satellite-derived heating rates for data assimilation within the tropics, *Mon. Weather Rev.*, **118**, 1743–1757.
- Hong, S. Y., and H. L. Pan (1996), Nonlocal boundary layer vertical diffusion in a Medium Range Forecast model, *Mon. Weather Rev.*, **124**, 2322–2339.
- Hou, A. Y., S. Q. Zhang, and O. Reale (2004), Variational continuous assimilation of TMI and SSM/I rain rates: Impact on GEOS-3 hurricane analysis and forecast, *Mon. Weather Rev.*, **132**, 2094–2109.

- Huang, X. Y., et al. (2009), Four-dimensional variational data assimilation for WRF: Formulation and preliminary results, *Mon. Weather Rev.*, 137, 299–314.
- Huffman, G. J., R. F. Adler, D. T. Bolvin, G. J. Gu, E. J. Nelkin, K. P. Bowman, Y. Hong, E. F. Stocker, and D. B. Wolff (2007), The TRMM multisatellite precipitation analysis (TMPA): Quasi-global, multiyear, combined-sensor precipitation estimates at fine scales, *J. Hydrometeorol.*, 8(1), 38–55.
- Joyce, R. J., J. E. Janowiak, P. A. Arkin, and P. Xie (2004), CMORPH: A method that produces global precipitation estimates from passive microwave and infrared data at high spatial and temporal resolution, *J. Hydrometeorol.*, 5, 487–503.
- Kain, J. S., and J. M. Fritsch (1993), Convective parameterization for mesoscale models: The Kain-Fritsch scheme, in *The Representation of Cumulus Convection in Numerical Models*, edited by K. A. Emanuel and D. J. Raymond, p. 246, Amer. Meteor. Soc., Boston, Mass.
- Krishnamurti, T. N., K. Ingles, S. Cooke, T. Kitade, and R. Pasch (1984), Details of low-latitude, medium-range numerical weather prediction using a global spectral model, Part 2: Effects of orography and physical initialization, *J. Meteorol. Soc. Jpn.*, 62, 613–648.
- Krishnamurti, T. N., J. Xue, H. S. Bedi, K. Ingles, and O. Oosterhof (1991), Physical initialization for numerical weather prediction over the tropics, *Tellus A*, 43, 53–81.
- Krishnamurti, T. N., H. S. Bedi, and K. Ingles (1993), Physical initialization using SSM/I rain rates, *Tellus A*, 45, 247–269.
- Kubota, T., et al. (2007), Global precipitation map using satelliteborne microwave radiometers by the GSMAp project: Production and validation, *IEEE Trans. Geosci. Remote Sens.*, 45(7), 2259–2275.
- Kumar, P., B. K. Bhattacharya, and P. K. Pal (2012), Impact of vegetation fraction from Indian geostationary satellite on short-range weather forecast, *Agric. For. Meteorol.*, 168, 82–92.
- Lopez, P. (2011), Direct 4D-Var assimilation of NCEP stage IV radar and gauge precipitation data at ECMWF, *Mon. Weather Rev.*, 139, 2098–2116.
- Marecal, V., and J.-F. Mahfouf (2000), Variational retrieval of temperature and humidity profiles from TRMM precipitation data, *Mon. Weather Rev.*, 128, 3853–3866.
- Marecal, V., and J. F. Mahfouf (2003), Experiments on 4D-Var assimilation of rainfall data using an incremental formulation, *Q. J. R. Meteorol. Soc.*, 129, 3137–3160.
- Mlawer, E. J., S. J. Taubman, P. D. Brown, M. J. Iacono, and S. A. Clough (1997), Radiative transfer for inhomogeneous atmosphere: RRTM, a validated correlated-k model for the longwave, *J. Geophys. Res.*, 102(D14), 16,663–16,682.
- Okamoto, K., T. Iguchi, N. Takahashi, K. Iwanami, and T. Ushio (2005), The global satellite mapping of precipitation (GSMAp) project, 25th IGARSS Proceedings, pp. 3414–3416.
- Parrish, D. F., and J. C. Derber (1992), The national meteorological center's spectral statistical interpolation analysis system, *Mon. Weather Rev.*, 120(8), 1747–1763.
- Prakash, S., and R. M. Gairola (2013), Validation of TRMM-3B42 precipitation product over the tropical Indian Ocean using rain gauge data from the RAMA buoy array, *Theor. Appl. Climatol.*, doi:10.1007/s00704-013-0903-3.
- Pu, Z., W.-K. Tao, B. Scott, J. Simpson, Y. Jia, J. Halverson, W. Olson, and A. Hou (2002), The impact of TRMM data on mesoscale numerical simulation of super typhoon, *Paka*. *Mon. Wea. Rev.*, 130, 2448–2458.
- Puri, K., and M. J. Miller (1990), The use of satellite data in the specification of convective heating for diabatic initialization and moisture adjustment in numerical weather prediction models, *Mon. Weather Rev.*, 118, 67–93.
- Rajeevan, M., J. Bhate, J. D. Kale, and B. Lal (2006), High resolution daily gridded rainfall data for the Indian region: Analysis of break and active monsoon spells, *Curr. Sci.*, 91, 296–306.
- Seto, S., N. Takahashi, and T. Iguchi (2005), Rain/no-rain classification methods for microwave radiometer observations over land using statistical information for brightness temperatures under no-rain conditions, *J. Appl. Meteorol.*, 44(8), 1243–1259.
- Singh, R., P. Kumar, and P. K. Pal (2012), Assimilation of oceansat-2 scatterometer derived surface winds in the Weather Research and Forecasting model, *IEEE Trans. Geosci. Remote Sens.*, 50(4), 1015–1021.
- Skamarock, W. C., J. B. Klemp, J. Dudhia, D. O. Gill, D. M. Barker, M. G. Duda, X. Y. Huang, W. Wang, and J. G. Powers (2008), A description of the advanced research WRF version 3, *Tech. Note NCAR/TN-475 STR*, pp. 113, Mesoscale and Microscale Meteorology Division, National Center of Atmospheric Research, June 2008.
- Treadon, R. E. (1996), Physical initialization in the NMC global assimilation system, *Meteorol. Atmos. Phys.*, 60, 57–86.
- Treadon, R. E. (1997), Assimilation of satellite derived precipitation estimates with the NCEP GDAS, PhD dissertation, The Florida State Univ., 348 pp.
- Tsuyuki, T. (1997), Variational data assimilation in the Tropics using precipitation data, Part III: Assimilation of SSM/I precipitation rates, *Mon. Weather Rev.*, 125, 1447–1464.
- Tustison, B., E. F. Georgiou, and D. Harris (2003), Scale-recursive estimation for multisensor Quantitative Precipitation Forecast verification: A preliminary assessment, *J. Geophys. Res.*, 108(D8), 8377, doi:10.1029/2001JD001073.
- Yuan, W., R. Yu, M. Zhang, W. Lin, H. Chen, and J. Li (2012), Regimes of diurnal variation of summer rainfall over subtropical East Asia, *J. Clim.*, 25, 3307–3320.
- Zou, X., and Y.-H. Kuo (1996), Rainfall assimilation through an optimal control of initial and boundary conditions in a limited-area mesoscale model, *Mon. Weather Rev.*, 124, 2859–2882.
- Zupanski, D., and F. Mesinger (1995), Four-dimensional variational assimilation of precipitation data, *Mon. Weather Rev.*, 123, 1112–1127.